

Fission of heavy Λ hypernuclei with the Skyrme-Hartree-Fock approach

F. Minato^a, S. Chiba^{a,b}, K. Hagino^c

^a*Japan Atomic Energy Agency, Tokai 319-1195, Japan*

^b*National Astronomical Observatory of Japan, Osawa, Mitaka, Tokyo 181-8588, Japan*

^c*Department of Physics, Tohoku University, Sendai 980-8578, Japan*

Abstract

Fission-related phenomena of heavy Λ hypernuclei are discussed with the constraint Skyrme-Hartree-Fock+BCS (SHF+BCS) method, in which a similar Skyrme-type interaction is employed also for the interaction between a Λ particle and a nucleon. Assuming that the Λ particle adiabatically follows the fission motion, we discuss the fission barrier height of $^{239}_{\Lambda}\text{U}$. We find that the fission barrier height increases slightly when the Λ particle occupies the lowest level. In this case, the Λ particle is always attached to the heavier fission fragment. This indicates that one may produce heavy neutron-rich Λ hypernuclei through fission, whose weak decay is helpful for the nuclear transmutation of long-lived fission products. We also discuss cases where the Λ particle occupies a higher single-particle level.

Key words: hypernuclei, fission, Skyrme-Hartree-Fock

PACS:

1. Introduction

Hyperons have attracted much interests since its discovery. The interaction between a hyperon (Y) and a nucleon (N) is important not only for understanding the mechanism of nuclear force but also for the equation of state of nuclear matter in astrophysical sites. YN scattering experiments have been difficult to perform since the life-time of hyperons in vacuum is so short (typically a few 10^{-10} seconds). Therefore, the information on the YN

Email address: minato.futoshi@jaea.go.jp (F. Minato)

interaction has been obtained mainly from the structure of finite hypernuclei, which are composed of neutrons, protons and at least one hyperon. There have been studied by now many single- Λ hypernuclei from H to U [1], and a few $\Lambda\Lambda$ and Σ hypernuclei have also been produced experimentally.

One of the important questions in hypernuclear physics is to clarify the role of hyperon in the structure of hypernuclei. An attractive YN force may cause a significant modification in the properties of a finite nucleus when a hyperon is added to it. Such impurity effect of hyperon for ${}^7_{\Lambda}\text{Li}$, that is, the shrinkage of ${}^6\text{Li}$ core in the hypernucleus, was predicted theoretically using the cluster models [2, 3, 4], which has subsequently been confirmed experimentally by Tanida *et al.* [5]. A recent theoretical work with the relativistic mean field (RMF) theory has also shown that the shape of ${}^{12}\text{C}$ and ${}^{28}\text{Si}$ changes from oblate to spherical when a Λ particle is added to them [6].

It is intriguing to ask whether the similar effects can be expected for heavy fissile nuclei. Interests in the fission of heavy Λ hypernuclei include i) a change of fission barrier height due to the additional Λ particle and ii) an attachment probability of a Λ particle to each fission fragments after fission takes place. The latter has been studied experimentally by Armstrong *et al.* for hypernuclei formed in anti-proton annihilation on ${}^{209}\text{Bi}$ and ${}^{238}\text{U}$ nuclei [7]. They reported that the Λ particle predominantly sticks to the heavier fission fragment. Theoretical works on the Λ attachment probability have been also performed in Refs. [8, 9, 10] with a phenomenological Woods-Saxon potential and the statistical method, yielding consistent results with the experiment finding. As for the former interest, to our knowledge, the fission barrier height of heavy hypernuclei has been studied neither theoretically nor experimentally.

The aim of this paper is then to clarify the impurity effects of Λ particle on the fission barrier height of heavy Λ hypernuclei and investigate a possibility to produce neutron-rich Λ hypernuclei, which are difficult to produce directly by experimental beams. To this end, we use the (constraint) Skyrme-Hartree-Fock+BCS (SHF+BCS) method. This method has been widely used for the study of fission [11, 12, 14, 15] and has been applied to hypernuclei as well [16, 17, 18, 19, 20, 21, 22]. It is also a virtue of this method that one can calculate the wave functions of Λ particle in a self-consistent manner.

The paper is organized as follows. In section 2, we describe the theoretical framework of the constraint SHF+BCS method. In section 3, we illustrate the potential energy surface for fission of heavy hypernuclei and

discuss an evolution of Λ particle motion during fission. In section 4, we give the conclusion and discuss possible applications of fission of heavy Λ hypernuclei.

2. Skyrme-Hartree-Fock method for hypernuclei

The Skyrme-Hartree-Fock method [13] has been extensively used for stable and unstable nuclei. In this approach, the effective NN interaction is described by the Skyrme interaction, which has the form of density-dependent zero-range interaction.

This method has been extended to hypernuclei [16], in which the ΛN and ΛNN interactions are also described by the similar Skyrme-like δ -interaction. The two-body ΛN interaction is given by,

$$\begin{aligned} v_{\Lambda N}(\vec{r}_\Lambda - \vec{r}_N) = & t_0^\Lambda (1 + x_0^\Lambda P_\sigma) \delta(\vec{r}_\Lambda - \vec{r}_N) \\ & + \frac{1}{2} t_1^\Lambda \left(\vec{k}'^2 \delta(\vec{r}_\Lambda - \vec{r}_N) + \delta(\vec{r}_\Lambda - \vec{r}_N) \vec{k}^2 \right) \\ & + t_2^\Lambda \vec{k}' \delta(\vec{r}_\Lambda - \vec{r}_N) \cdot \vec{k} + i W_0^\Lambda \vec{k}' \delta(\vec{r}_\Lambda - \vec{r}_N) \cdot (\sigma \times \vec{k}), \end{aligned} \quad (1)$$

while the three-body ΛNN interaction is,

$$v_{\Lambda NN}(\vec{r}_\Lambda, \vec{r}_1, \vec{r}_2) = t_3^\Lambda \delta(\vec{r}_\Lambda - \vec{r}_1) \delta(\vec{r}_\Lambda - \vec{r}_2). \quad (2)$$

Here, \vec{k} and \vec{k}' are the derivative operators acting on the right and the left hand sides, respectively. The parameters in Eqs. (1) and (2) have been adjusted to fit the experimental binding energies of Λ hypernuclei [16, 17]. With these effective interactions, the total energy E of hypernucleus is given by,

$$E = E_N + E_\Lambda \quad (3)$$

$$E_N = \int H_N(\vec{r}) d\vec{r} + E_N^{\text{pair}} \quad (4)$$

$$E_\Lambda = \int H_\Lambda(\vec{r}) d\vec{r},$$

where E_N , E_Λ , and E_N^{pair} are the energy of the core nucleus, that of the Λ particle, and the pairing energy, respectively. The energy density for the core nucleus, $H_N(\vec{r})$, is standard and its explicit form can be found *e.g.*, in

Refs.[13, 14]. The energy density for the Λ particle, $H_\Lambda(\vec{r})$, is given by,

$$\begin{aligned}
H_\Lambda(\vec{r}) &= \frac{\hbar^2}{2m_\Lambda} \tau_\Lambda + t_0^\Lambda \left(1 + \frac{1}{2} x_0^\Lambda\right) \rho \rho_\Lambda + \frac{1}{4} (t_1^\Lambda + t_2^\Lambda) (\tau_\Lambda \rho + \tau \rho_\Lambda) \\
&+ \frac{1}{4} (3t_1^\Lambda - t_2^\Lambda) (\vec{\nabla} \rho \cdot \vec{\nabla} \rho_\Lambda) + \frac{1}{2} W_0^\Lambda (\vec{\nabla} \rho \cdot \vec{J}_\Lambda + \vec{\nabla} \cdot \vec{J}) \\
&+ \frac{1}{4} t_3^\Lambda \rho_\Lambda (\rho^2 + 2\rho_n \rho_p),
\end{aligned} \tag{5}$$

where $\rho = \rho(\vec{r}) = \rho_p(\vec{r}) + \rho_n(\vec{r})$, $\tau = \tau(\vec{r}) = \tau_p(\vec{r}) + \tau_n(\vec{r})$, and $\vec{J} = \vec{J}(\vec{r}) = \vec{J}_p(\vec{r}) + \vec{J}_n(\vec{r})$ are the number, the kinetic energy, and the spin-current densities for the core nucleus, respectively. $\rho_\Lambda = \rho_\Lambda(\vec{r})$, $\tau_\Lambda = \tau_\Lambda(\vec{r})$, and $\vec{J}_\Lambda = \vec{J}_\Lambda(\vec{r})$ are the same quantities, but for the Λ particle.

The single-particle wave functions $\phi(\vec{r})$ are obtained by minimizing the total energy E . This leads to the SHF equations for proton ($q = p$) and neutron ($q = n$) given by

$$\left(-\vec{\nabla} \cdot \frac{\hbar^2}{2m_q^*(\vec{r})} \vec{\nabla} + U_q(\vec{r}) + U_q^\Lambda(\vec{r}) \right) \phi_q(\vec{r}) = \epsilon_q \phi_q(\vec{r}), \tag{6}$$

where $m_q^*(\vec{r})$ is the nucleon effective mass defined as,

$$\frac{\hbar^2}{2m_q^*(\vec{r})} = \frac{\hbar^2}{2m_q} + \frac{1}{4} (t_1 + t_2) \rho(\vec{r}) + \frac{1}{8} (t_2 - t_1) \rho_q(\vec{r}) + \frac{1}{4} (t_1^\Lambda + t_2^\Lambda) \rho_\Lambda(\vec{r}). \tag{7}$$

$U_q^\Lambda(\vec{r})$ is the mean-field potential due to the ΛN interaction given by,

$$\begin{aligned}
U_q^\Lambda(\vec{r}) &= t_0^\Lambda \left(1 + \frac{1}{2} x_0^\Lambda\right) \rho_\Lambda(\vec{r}) + \frac{1}{4} (t_1^\Lambda + t_2^\Lambda) \tau_\Lambda(\vec{r}) - \frac{1}{4} (3t_1^\Lambda - t_2^\Lambda) \vec{\nabla}^2 \rho_\Lambda(\vec{r}) \\
&- \frac{1}{2} W_0^\Lambda (\vec{\nabla} \vec{J}_\Lambda(\vec{r})) + \frac{1}{2} W_0^\Lambda \vec{\nabla} \rho_\Lambda(\vec{r}) (-i) (\vec{\nabla} \times \vec{\sigma}) + \frac{1}{2} t_3^\Lambda \rho_\Lambda(\vec{r}) (\rho(\vec{r}) + \rho_q(\vec{r})).
\end{aligned} \tag{8}$$

Similarly, the wave function for the Λ particle is obtained with the equation,

$$\left(-\vec{\nabla} \cdot \frac{\hbar^2}{2m_\Lambda^*(\vec{r})} \vec{\nabla} + U_\Lambda^N(\vec{r}) \right) \phi_\Lambda(\vec{r}) = \epsilon_\Lambda \phi_\Lambda(\vec{r}), \tag{9}$$

where $m_\Lambda^*(\vec{r})$ are the Λ effective mass defined as,

$$\frac{\hbar^2}{2m_\Lambda^*(\vec{r})} = \frac{\hbar^2}{2m_\Lambda} + \frac{1}{4} (t_1^\Lambda + t_2^\Lambda) \rho(\vec{r}). \tag{10}$$

The mean-field potential U_Λ^N for the Λ particle is given by,

$$\begin{aligned}
U_\Lambda^N(\vec{r}) = & t_0^\Lambda \left(1 + \frac{1}{2} x_0^\Lambda \right) \rho(\vec{r}) + \frac{1}{4} (t_1^\Lambda + t_2^\Lambda) \tau(\vec{r}) - \frac{1}{4} (3t_1^\Lambda - t_2^\Lambda) \vec{\nabla}^2 \rho(\vec{r}) \\
& + \frac{1}{2} W_0^\Lambda \vec{\nabla} \rho(\vec{r}) (-i) (\vec{\nabla} \times \vec{\sigma}) - \frac{1}{2} W_0^\Lambda \vec{\nabla} \vec{J}(\vec{r}) + \frac{1}{4} t_3^\Lambda \left(\rho^2(\vec{r}) + 2\rho_n(\vec{r})\rho_p(\vec{r}) \right).
\end{aligned} \tag{11}$$

We define the quadrupole operator as,

$$\hat{Q}_2^q = \sqrt{\frac{16\pi}{5}} \sum_{i \in q} r_i^2 Y_{20}(\theta_i), \tag{12}$$

and the octupole operator as,

$$\hat{Q}_3^q = \sum_{i \in q} r_i^3 Y_{30}(\theta_i), \tag{13}$$

respectively ($q = p, n, \Lambda$). Using the self-consistent solution of the SHF equations, the multipole moments are calculated as,

$$Q_2^q = \sqrt{\frac{16\pi}{5}} \int d\vec{r} r^2 Y_{20}(\theta) \rho_q(\vec{r}), \tag{14}$$

$$Q_3^q = \int d\vec{r} r^3 Y_{30}(\theta) \rho_q(\vec{r}), \tag{15}$$

for the quadrupole and octupole, respectively.

We perform our calculations by modifying the computer code `SKYAX` [23, 24]. This code solves the SHF equations in the coordinate space assuming axial symmetry for the nuclear shape. The potential energy surface for fission is obtained by constraining on the quadrupole moment, while the octupole moment is optimized by adding a small octupole moment to the initial wave functions. We take the mesh size of $\Delta r = \Delta z = 1.0$ fm with boundary conditions of vanishing wave functions at $r = 20$ fm, $z = -25$ fm, and $z = 25$ fm, where $r = \sqrt{x^2 + y^2}$.

The pairing correlation among nucleons is treated in the BCS approximation. We use the density-dependent contact interaction,

$$v_{\text{pair}}^q(\vec{r}_1, \vec{r}_2) = v_0^q \left(1 - \frac{\rho(\vec{r})}{\rho_0} \right) \delta(\vec{r}_1 - \vec{r}_2), \tag{16}$$

for the pairing interaction. In the code, a smooth cut-off function [25]

$$f_k = \frac{1}{1 + \exp((\epsilon_k - \lambda - \Delta E)/\mu)} \quad (17)$$

is introduced for the pairing active space. Here, λ is the Fermi energy, and ΔE is determined so that

$$N_{\text{act}} = \sum_k f_k = N_q + 1.65N_q^{2/3} \quad (18)$$

with $\mu = \Delta E/10$, N_q being the number of proton or neutron. The pairing energy is given by,

$$E_N^{\text{pair}} = \sum_{k \in p, n} u_k v_k \Delta_k f_k, \quad (19)$$

where u_k and v_k are the uv factor in the BCS approximation, and Δ_k is the pairing gap.

3. Results

Heavy Λ hypernuclei, which are produced by (K^-, π^-) , (π^+, K^+) , or $(e, e'K^+)$ reactions, are initially at an excited state. Then the fission channel competes with several other decay channels. Three fission processes can be considered: (I) the Λ particle itself decays via non-mesonic decay followed by fission of the remaining nucleus, (II) fission occurs after the Λ particle de-excites to the lowest single-particle state emitting several γ -rays, (III) fission occurs while the Λ particle is at an excited single-particle level. Among them, the process (I) corresponds to a statistical fission of an excited nucleus and we do not consider it in this work.

We calculate the potential energy curve of $^{239}_{\Lambda}\text{U}$ as a function of $Q_2 = Q_2^p + Q_2^n + Q_2^{\Lambda}$, and compare it with that of ^{238}U . We set the pairing strength parameters to be $v_0^p = 1410.0 \text{ MeV}\cdot\text{fm}^3$ for proton and $v_0^n = 910.0 \text{ MeV}\cdot\text{fm}^3$ for neutron so as to reproduce the empirical pairing gap of ^{238}U , that is, $\Delta_n = 0.674 \text{ MeV}$ and $\Delta_p = 1.168 \text{ MeV}$ obtained with the three-point formula for nuclear mass. We adopt the parameter set SkM* [11] for the NN interaction, while the parameter No. 4 in Table. I of Ref. [17] for the ΛN interaction, which is optimized to $^{209}_{\Lambda}\text{Pb}$,

$$\begin{aligned} t_0^{\Lambda} &= -253.500 \text{ MeV}\cdot\text{fm}^3, & x_0^{\Lambda} &= -0.216, & t_1^{\Lambda} &= 76.920 \text{ MeV}\cdot\text{fm}^5, \\ t_2^{\Lambda} &= 28.080 \text{ MeV}\cdot\text{fm}^5, & t_3^{\Lambda} &= 0.000 \text{ MeV}\cdot\text{fm}^6, & W_0^{\Lambda} &= 0.000 \text{ MeV}\cdot\text{fm}^5. \end{aligned}$$

	^{238}U	$^{239}_{\Lambda}\text{U}$
$B_f(\text{inner})$ (MeV)	8.20	8.47
$B_f(\text{outer})$ (MeV)	6.60	7.42

Table 1: The height of the inner and outer fission barriers for the ^{238}U and $^{239}_{\Lambda}\text{U}$ nuclei when the Λ particle occupies the lowest single-particle state during fission.

We have confirmed that the potential energy curve of $^{239}_{\Lambda}\text{U}$ does not alter significantly even when other parameter sets for the ΛN interaction [16, 17] are employed.

3.1. Λ at the lowest single-particle level

Let us first discuss the fission of hypernucleus $^{239}_{\Lambda}\text{U}$ at the ground state. For this purpose, we assume that a Λ particle follows adiabatically the fission motion. That is, the Λ particle is at the lowest single-particle level at every instant. Fig. 1 shows the fission barrier for ^{238}U (the dashed line) and $^{239}_{\Lambda}\text{U}$ (the solid line) as a function of total quadrupole moment Q_2 . Those curves are shifted so that the ground state configuration has zero energy. The deformation parameter for the ground state does not change significantly by adding a Λ particle. On the other hand, the fission barrier height of $^{239}_{\Lambda}\text{U}$ slightly increases as compared to that of ^{238}U . This suggests that ^{238}U may become more stable by adding a Λ particle, although one needs to evaluate also the effect of Λ particle on the mass inertia to reach a definite conclusion. We list the height of the inner and outer fission barriers in Tab. 1. The inner barrier height increases by about 0.27 MeV, while the outer barrier by about 0.82 MeV due to the additional Λ particle in the $^{239}_{\Lambda}\text{U}$ nucleus.

The degree of increase of the fission barrier height is primarily determined by the energy of Λ particle, E_{Λ} . The fission barrier height is defined as the energy difference at the saddle point configuration (s.p.) and the ground state (g.s.). This reads

$$\begin{aligned}
 B_f &= E(\text{s.p.}) - E(\text{g.s.}) \\
 &= \left(E_N(\text{s.p.}) - E_N(\text{g.s.}) \right) + \left(E_{\Lambda}(\text{s.p.}) - E_{\Lambda}(\text{g.s.}) \right).
 \end{aligned}
 \tag{20}$$

The first and second terms in Eq. (20) correspond to the energy difference for the core nucleus and the Λ particle, respectively. We plot these quantities as a function of Q_2 in Fig. 2. The top panel shows $E_N - E_N(\text{g.s.})$ for

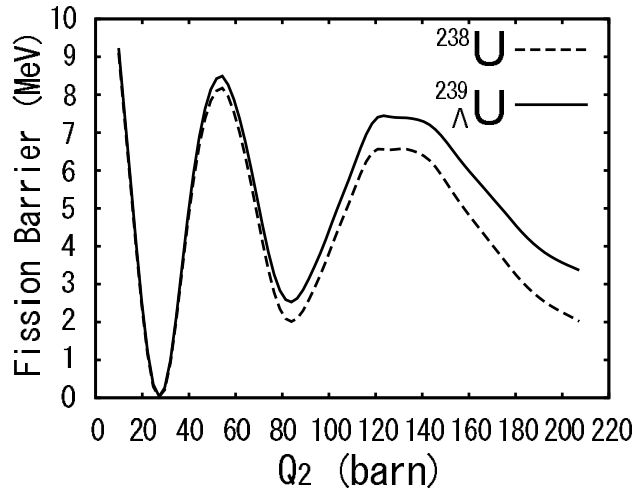


Figure 1: The fission barrier of ^{238}U (the dotted line) and $^{239}_{\Lambda}\text{U}$ (the solid line) nuclei obtained with the Skyrme-Hartree-Fock method. The Λ particle is assumed to occupy the lowest single-particle state during fission. The energy curves are shifted so that the ground state configuration has zero energy.

^{238}U (the solid line) and $^{239}_{\Lambda}\text{U}$ (the dashed line). Notice that the difference between these two curves is small, as shown in the middle panel in Fig. 2. The difference is in fact about the order of 1% of the barrier height, and thus we conclude that the energy of the core nucleus is insensitive to the presence of Λ particle. In contrast, the energy of the Λ particle, E_{Λ} , varies more significantly as a function of Q_2 . The bottom panel in Fig. 2 shows $E_{\Lambda} - E_{\Lambda}(\text{g.s.})$ as a function of Q_2 . The energy E_{Λ} monotonically increases with the quadrupole moment Q_2 with respect to the ground state. The energy difference is $\Delta E_{\Lambda} = E_{\Lambda}(\text{s.p.}) - E_{\Lambda}(\text{g.s.}) = 0.25$ MeV at the inner barrier position, which almost amounts to the increase of the fission barrier height ($\Delta B_f = 0.27$ MeV). It is thus evident that the change in the fission barrier height is dominantly resulted from the energy of the Λ particle.

Fig. 3 shows the density distributions for the core nucleus ^{238}U (the left panels) in $^{239}_{\Lambda}\text{U}$ and the Λ particle (the right panels) at the ground state ($Q_2 = 27.15$ b), the second minimum ($Q_2 = 83.90$ b), the outer saddle point ($Q_2 = 123.39$ b), and $Q_2 = 200.00$ b. At $Q_2 = 200$ b, the core nucleus is separated asymmetrically into two nuclei, where the fragment on the left-hand side is heavier than that on the right-hand side (the initial octupole moment at the first stage of iteration determines which fragment is heavier).

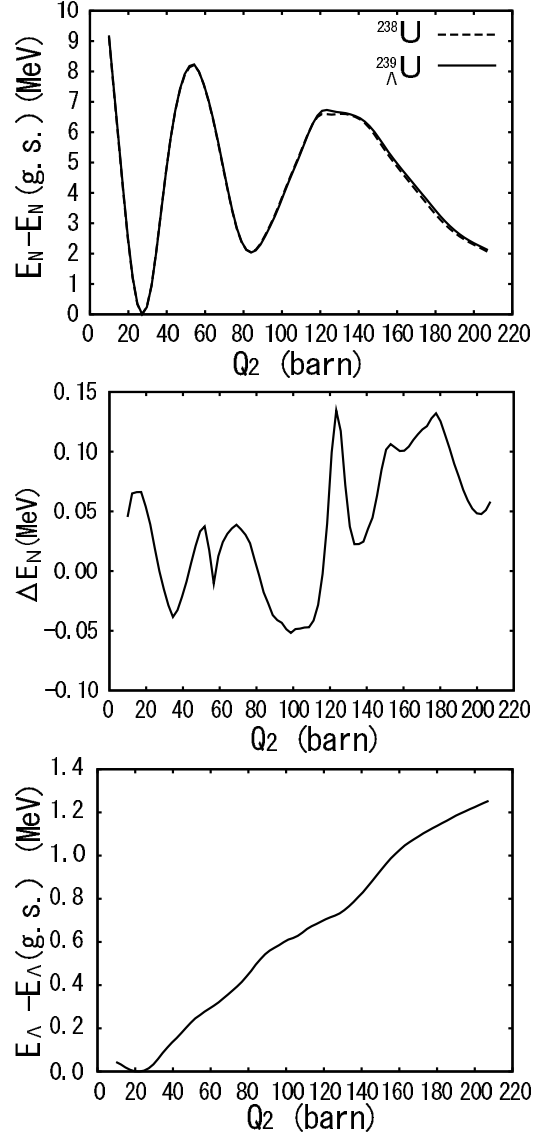


Figure 2: (The top panel:) The energy of the core nucleus E_N for the ^{238}U (the solid line) and $^{239}_{\Lambda}\text{U}$ (the dashed line) nuclei as a function of the total quadrupole moment Q_2 . The Λ particle is assumed to be at the lowest single-particle state. (The middle panel:) The difference between the solid and the dashed curves in the upper left panel. (The bottom panel:) The energy of the Λ particle E_{Λ} for $^{239}_{\Lambda}\text{U}$ with respect to that for the ground state as a function of Q_2 .

We see that the Λ particle is localized in the region of $z < 0$, that is, it is stuck to the heavier fission fragment. This is a natural consequence of the fact that the binding energy for the Λ particle is larger in the heavier nucleus.

Notice that the ΛN attractive interaction can attract more nucleons in the heavier fission fragment. In order to see this effect, we plot in Fig. 4 the difference between the density of the core nucleus ^{238}U in $^{239}_{\Lambda}\text{U}$ and the density of ^{238}U in the absence of the Λ particle at $Q_2 = 200$ barn. That is,

$$\Delta\rho(\vec{r}) = \rho_{\text{core}}^{\Lambda}(\vec{r}) - \rho(\vec{r}), \quad (21)$$

where $\rho_{\text{core}}^{\Lambda}(\vec{r})$ is the density of ^{238}U in $^{239}_{\Lambda}\text{U}$ and $\rho(\vec{r})$ is the density of ^{238}U without the Λ particle. As shown in Fig. 3, the left hand side ($z < 0$) corresponds to the heavier fragment, to which the Λ particle is stuck. We can see that $\Delta\rho(\vec{r})$ is positive (red) on the left side, and nucleons are actually attracted into the heavier fragment by the presence of Λ particle. If we integrate the region of $z < 0$, about 0.54 proton and 0.86 neutrons are attracted due to the Λ particle.

The motion of the Λ particle during fission can also be inferred from the single-particle levels for the Λ particle. We plot them in Fig. 5 as a function of Q_2 . The lowest level (the thick solid line) does not cross with other levels in the region which we consider, and the interaction between the lowest level and the others is small. This fact validates the adiabatic approximation to a large extent. Notice that each single-particle level is smoothly connected to those of two isolated fission fragments at large Q_2 . In particular, the lowest level is connected to the lowest level of the heavier fragment because the Λ binding energy is larger in the heavier fragment. As a consequence, the Λ particle is always stuck to the heavier fission fragment when it is at the lowest single-particle level.

3.2. Λ at a higher single-particle level

Let us next discuss the fission process when a Λ particle is at a higher single-particle level. This corresponds to the case where the hypernucleus goes to fission before the Λ particle produced experimentally, which is at first at an excited state, deexcites to the lowest level. For this purpose, we select four single-particle levels with $K = 1/2$ around the neutron Fermi energy, K being the projection of the single-particle angular momentum onto the symmetry axis. Those four levels are denoted as level A, B, C, and D in Fig. 6 by the thick solid lines. As in the previous subsection, we assume that Λ particle adiabatically moves at the level crossing points.

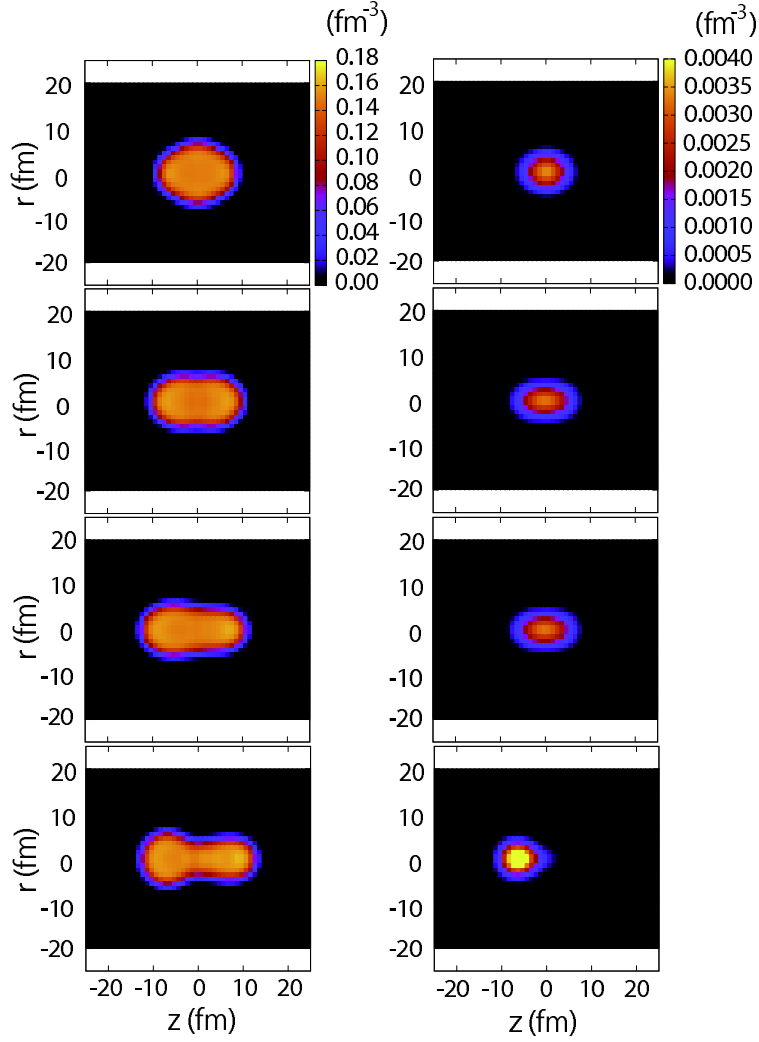


Figure 3: The density distribution for the core nucleus (the left panels) and the Λ particle (the right panels) in $^{239}_{\Lambda}\text{U}$ at the ground state ($Q_2 = 27.15$ b), the second minimum ($Q_2 = 83.90$ b), the outer saddle point ($Q_2 = 123.39$ b), and $Q_2 = 200$ b. The Λ particle is put at the lowest single particle level at all the deformations.

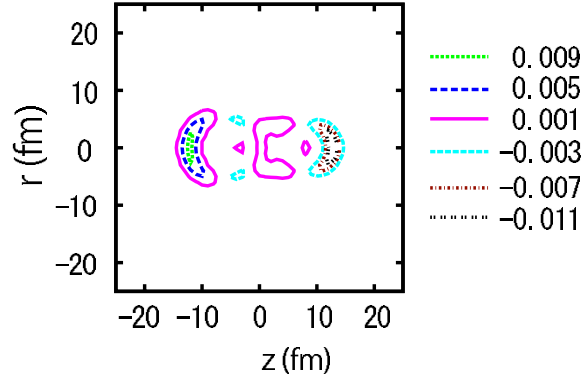


Figure 4: The difference between the density of the core nucleus ^{238}U in $^{239}_{\Lambda}\text{U}$ and the density of ^{238}U in the absence of the Λ particle at $Q_2 = 200$ barn.

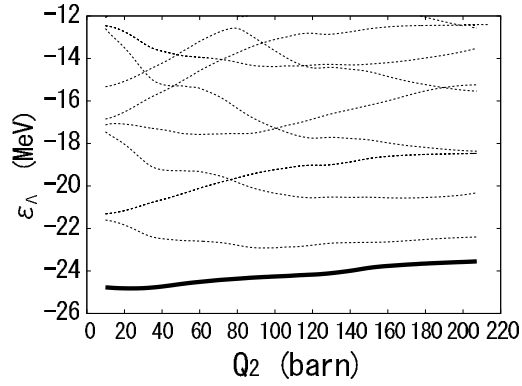


Figure 5: Single-particle levels for the Λ particle in $^{239}_{\Lambda}\text{U}$ as a function of Q_2 . We assume that the Λ particle stays at the lowest level (the thick solid line) at all the deformations.

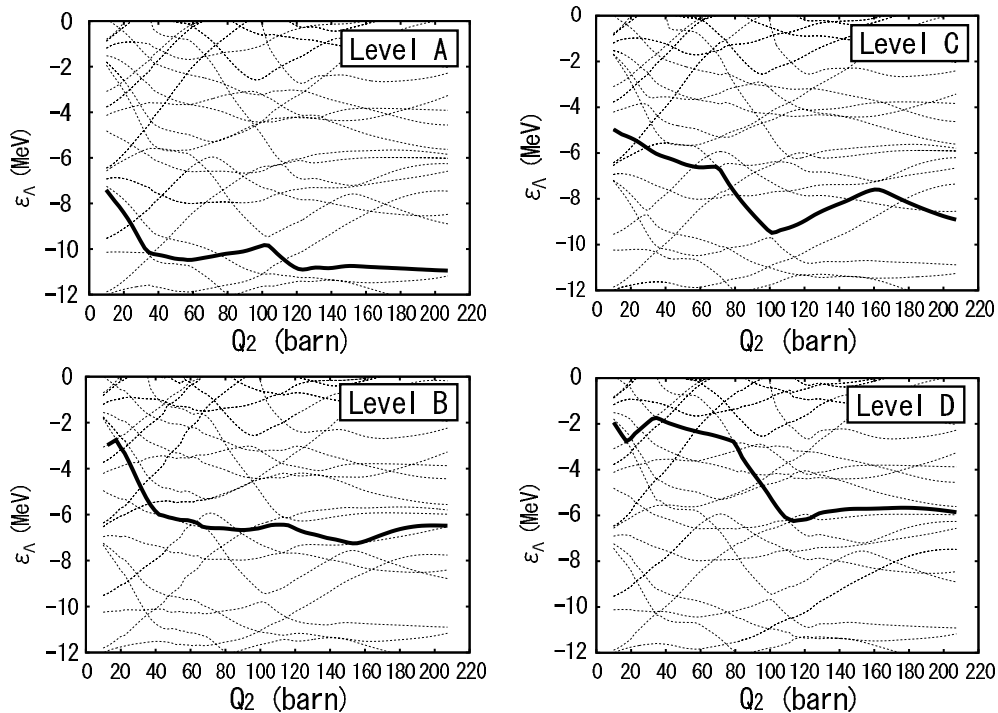


Figure 6: Same as Fig. 5, but for the cases when the Λ particle is at four different $K=1/2$ levels denoted by the thick solid lines.

The resultant fission barrier curves for each configuration are shown in Fig. 7. The height for the inner and outer barriers is listed in Tab. 2. The fission barrier heights for all the cases are lower than that for ^{238}U shown in Fig. 1 (see also Table 1). As we argued in the previous subsection, these changes of the barrier height with respect to the barrier height for the core nucleus ^{238}U are intimately connected to the behaviour of Λ single-particle energies. In Fig. 6, one notices that the single-particle energies for the occupied levels decrease away from the ground state ($Q_2 = 27.15$ b), leading to the decrease of fission barrier height.

In order to see to which fragment the Λ particle is stuck when it is at an excited level, we plot the Λ densities for the levels A, B, C, and D at $Q_2 = 200$ b in Fig. 8. We have confirmed that the density distribution for the core nucleus is almost the same as that with Λ at the lowest level shown in Fig. 3. In Fig. 8, one sees that the Λ particle is attracted by the heavier

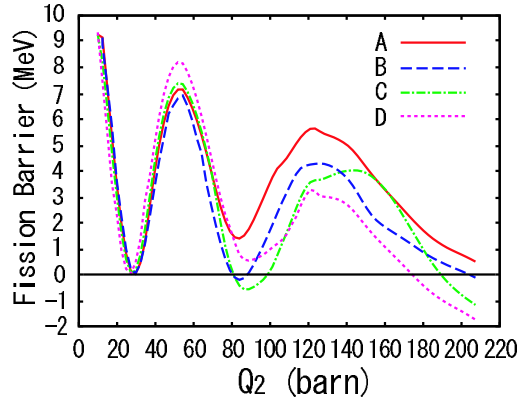


Figure 7: Fission barrier for the $^{239}_{\Lambda}\text{U}$ nucleus as a function of the total quadrupole moment Q_2 when the Λ particle occupies the four different single-particle levels denoted by the thick solid line in Fig. 5.

	(A)	(B)	(C)	(D)
$B_f(\text{inner})$ (MeV)	7.12	6.87	7.31	8.16
$B_f(\text{outer})$ (MeV)	5.61	4.25	3.95	3.23

Table 2: The height of the inner and outer fission barriers for the $^{239}_{\Lambda}\text{U}$ nucleus for the Λ particle configurations shown in Fig. 6.

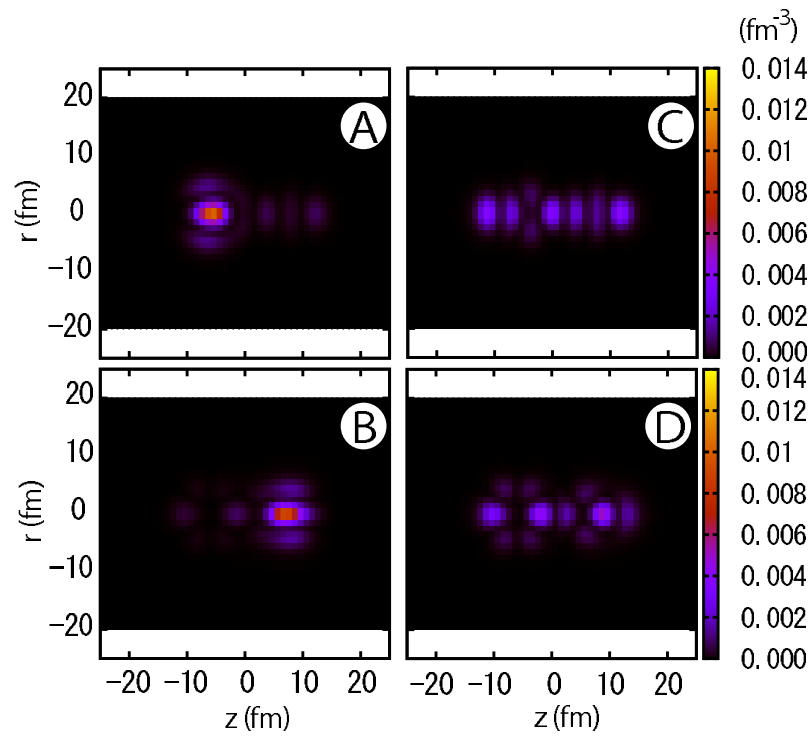


Figure 8: The density distribution for the Λ particle at $Q_2 = 200$ b for the configurations A , B , C , and D .

fragment ($z < 0$) for the level A, similar to the case of Λ particle at the lowest single-particle level. On the other hand, the Λ particle moves to the lighter fragment ($z > 0$) in the case of level B. For the levels C and D, the density distribution is not localized and we cannot say to which fragment the Λ particle moves.

Fig. 9 shows the Λ mean-field potential $U_{\Lambda}^N(\vec{r})$ (the solid line) and the Λ wave functions $\phi_{\Lambda}(r, z)$ (the dashed line) at $Q_2 = 200$ barn for the lowest, A, B, C, and D levels. These are plotted for three different values of r , that is, $r=0$ fm, 2 fm, and 4 fm. The localization of the Λ wave function for the lowest level, the levels A and B are clearly seen. For the levels C and D, the wave function is expected to be localized more clearly at larger values of quadrupole moment Q_2 , after a few more level crossings, although we are unable to check it numerically because of a difficulty of numerical calculation at large deformations.

4. Conclusion

We have calculated the fission barrier curve for ${}^{239}_{\Lambda}\text{U}$ hypernucleus with the constraint Skyrme-Hartree-Fock + BCS method and compared it with that for ${}^{238}\text{U}$. For this purpose, we have assumed that the Λ particle adiabatically follows the fission process. We found that the fission barrier height increases when a Λ particle is added to the lowest single-particle level of ${}^{239}_{\Lambda}\text{U}$. We argued that this is caused because the the lowest Λ single-particle energy increases towards the saddle point. On the other hand, we have confirmed that, when the single-particle energy decreases at the saddle point as compared to the ground state, the fission barrier height with that configuration decreases. We also discussed the effect of Λ particle on the mass partition of fission fragments. We have shown that the mass of the fragment to which the Λ particle is attached increases due to the attractive interaction between Λ and nucleons.

The adiabatic approximation which we employed in this paper would be justified when the Λ particle occupies the lowest single-particle level. For a Λ particle at an excited state, on the other hand, its validity depends on how fast the fission takes place. When the fission takes place rapidly, the Λ particle may diabatically follow the fission process. In order to take into account the deviation from the adiabatic approximation, a dynamical calculation for fission with the Landau-Zener transition at level crossings is called for.

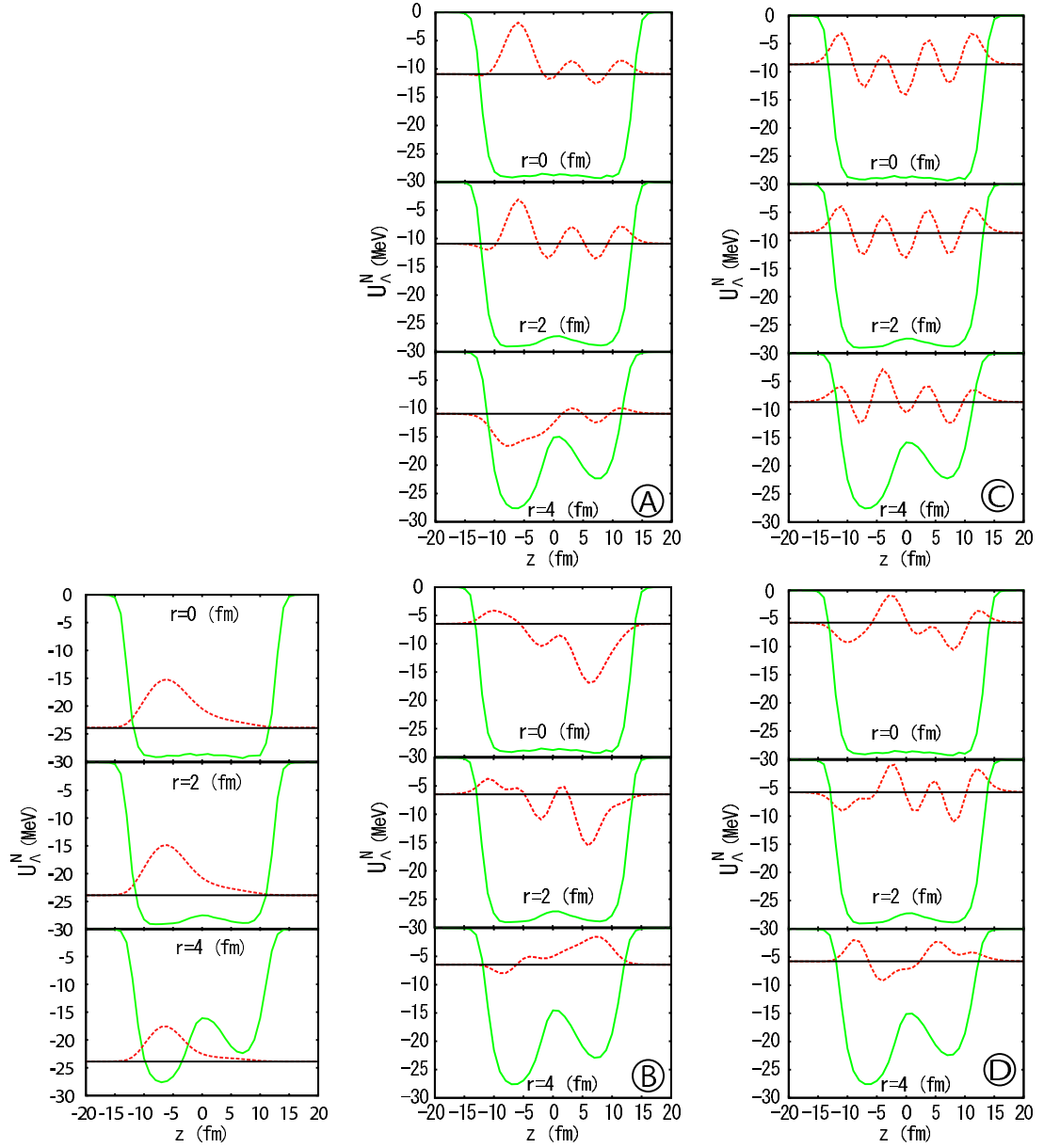


Figure 9: The mean-field potential for the Λ particle, $U_{\Lambda}^N(\vec{r})$, (the solid line) and the Λ wave function, $\phi_{\Lambda}(r, z)$, (the dashed line) at $r=0, 2$, and 4 fm and at the total quadrupole moment of $Q_2 = 200$ barn for the lowest (the left bottom panel), A, B, C, and D levels.

Lastly, we would like to point some possible applications of the fission of heavy Λ hypernuclei. One is a possibility to produce heavy neutron-rich Λ hypernuclei. A light neutron-rich hypernucleus ${}^{\Lambda}_{10}\text{Li}$ has been successfully produced via (π^-, K^+) reaction [26, 27]. This reaction converts two protons to a Λ and a neutron. It is therefore difficult with this method to produce a hypernucleus far from the stability line in the heavy mass region. In contrast, since the Λ particle eventually emerges in one of the fission fragments, the fission of heavy Λ hypernuclei may open up a novel method to produce a heavy neutron-rich Λ hypernucleus. Notice that heavy neutron-rich nuclei (without hyperon) has been produced via in-flight fission of ${}^{238}\text{U}$ at new generation radioactive isotope beam facilities[28, 29]. Another application of fission of heavy Λ hypernuclei is the nuclear transmutation. If a Λ particle remains at a fission fragment, it eventually decays by weak interaction (predominantly by non-mesonic decay). The weak decay of Λ induces fission, and/or neutron and proton emissions of the fission fragment which the Λ particle originally sticks to[30, 31]. It is an interesting future question whether such processes can be utilized to transmute long-lived radioactive wastes produced at nuclear power plants.

Acknowledgement

We thank Myaing Thi Win, E. Hiyama, and S. Hirenzaki for useful discussions. This work was supported by the Japanese Ministry of Education, Culture, Sports, Science and Technology by Grant-in-Aid for Scientific Research under the program number 19740115.

References

- [1] O. Hashimoto and H. Tamura, Prog. Part. Nucl. Phys. **57**, (2006) 564.
- [2] T. Motoba, H. Bando, and K. Ikeda, Prog. Theor. Phys. **70**, (1983) 189.
- [3] E. Hiyama et al., Phys. Rev. C **53**, (1996) 2075.
- [4] E. Hiyama, M. Kamimura, K. Miyazaki, and T. Motoba, Phys. Rev. C **59**, (1999) 2351.
- [5] K. Tanida et al., Phys. Rev. Lett., **86** (2001) 1982.
- [6] Myaing Thi Win, and K. Hagino Phys. Rev. C **79** (2009) 054311.

- [7] T.A.Armstrong, J.P.Bocquet, G.Ericsson, et al. Phys. Rev. C **47** (1993) 1957.
- [8] H.J. Krappe and V.V. Pashkevich, Phys. Rev. C **47** (1993) 1970.
- [9] F.F. Karpeshin, C.G. Koutroulos, M.E. Grypeos, Nucl. Phys. **A595** (1995) 209.
- [10] H.J. Krappe and V.V. Pashkevich, Phys. Rev. C **53** (1996) 1025.
- [11] J. Bartel, P. Quentin, M. Brack, C. Guet, and H.-B. Hakansson, Nucl. Phys. **A635**, (1982) 231.
- [12] J.A. Sheikh, W. Nazarewicz, J.C. Pei Phys. Rev. C **80** (2009) 011302.
- [13] D. Vautherin and D.M. Brink, Phys. Rev. C **5**, (1972) 626.
- [14] F. Minato and K. Hagino, Phys. Rev. C **77** (2008) 044308.
- [15] M. Bender, R.H. Heenen Phys. Rev. C **70** (2004) 054304.
- [16] M. Rayet, Nucl. Phys. **A367** (1981) 381; Ann. of Phys. **102** (1976) 226.
- [17] Y. Yamamoto, H. Bando, and J. Zofka, Prog. Theor. Phys. **80**, (1988) 757.
- [18] Y. Yamamoto, H. Bando, Prog. Theor. Phys. **83**, (1990) 254.
- [19] D.E. Lanskoy and Y. Yamamoto, Phys. Rev. C **55**, (1997) 2330.
- [20] D.E. Lanskoy, Phys. Rev. C **58**, (1998) 3351.
- [21] J. Cugnon, A. Lejeune, and H.-J. Schulze, Phys. Rev. C **62** (2000) 064308.
- [22] I. Vidaña, A. Polls, A. Ramos, and H.-J. Schulze, Phys. Rev. C **64** (2001) 044301.
- [23] P.-G. Reinhard, the computer code SKYAX (unpublished).
- [24] P.-G. Reinhard, D.J. Dean, W. Nazarewicz, J. Dobaczewski, J.A. Maruhn, and M.R. Strayer, Phys. Rev. C **60**, (1999) 014316.

- [25] M. Bender, K. Rutz, P.-G. Reinhard, J.A. Maruhn, and W. Greiner, Phys. Rev. C **58**, (1998) 2126.
- [26] P.K. Saha *et al.*, Phys. Rev. Lett. **94**, (2005) 052502.
- [27] H. Tamura, Int. J. of Mod. Phys. A**24**, (2009) 2101.
- [28] T. Ohnishi *et al.*, J. of Phys. Soc. of Japan, **77** (2008) 083201.
- [29] C.M. Folden III *et al.*, Phys. Rev. C**79** (2009) 064318.
- [30] H. Ohm *et al.*, Phys. Rev. C**55** (1997) 3062.
- [31] P. Kulesa *et al.*, Phys. Lett. **B427** (1998) 403.